# Effect of columnar defects on the vortex-solid melting transition in $Bi_2Sr_2CaCu_2O_8$

B. Khaykovich

*Department of Condensed Matter Physics, The Weizmann Institute of Science, 76100 Rehovot, Israel*
*and CNRS, URA 1380, Laboratoire des Solides Irradiés, École Polytechnique, 91128 Palaiseau, France*

M. Konczykowski

*CNRS, URA 1380, Laboratoire des Solides Irradiés, École Polytechnique, 91128 Palaiseau, France*

K. Teitelbaum

*Department of Condensed Matter Physics, The Weizmann Institute of Science, 76100 Rehovot, Israel*
*and Kazan State University, Kazan 420008, Russia*

E. Zeldov and H. Shtrikman

*Department of Condensed Matter Physics, The Weizmann Institute of Science, 76100 Rehovot, Israel*

M. Rappaport

*Physics Services, The Weizmann Institute of Science, 76100 Rehovot, Israel*
(Received 20 January 1998)

The first-order phase transition of the vortex-lattice in $Bi_2Sr_2CaCu_2O_8$ crystals is shown to transform into a continuous transition when disorder is introduced via a very low concentration of columnar defects. We demonstrate fine tuning of the disorder strength and the recovery of the first-order transition by varying the concentration of the columns, by changing the temperature along the melting line, or by tilting the magnetic field with respect to the columns. [S0163-1829(98)52522-2]

The interaction of vortices in high-temperature superconductors (HTSC) with columnar defects is the subject of numerous recent investigations.[1–11] The interplay between the different energy scales due to pinning, vortex-vortex interactions, and thermal fluctuations results in very complicated vortex dynamics and gives rise to a rich vortex matter phase diagram, the exact structure of which is as yet unclear. In particular, the first-order vortex-lattice melting transition (FOT) occurs when the energy of thermal fluctuations becomes comparable to the elastic energy of the solid vortex lattice.[1,12,13] This transition is observed only in very clean crystals in which the pinning energy is much smaller than the elastic and thermal energies at the transition. Due to the practical interest, most of the studies of columnar defects are carried out at substantial irradiation doses.[3–9] In this case, the vortex solid is a disordered Bose-glass phase, which is governed by the pinning energy rather than by the elastic energy, and it melts through a continuous transition.[2,10] In this paper, in contrast, we study the effect of very low concentrations of columnar defects which act as weak correlated disorder in $Bi_2Sr_2CaCu_2O_8$ (BSCCO) crystals. The chosen concentrations are such that the pinning energy is comparable to the elastic and thermal energies at the transition, so that the appearance and disappearance of the FOT could be tuned by varying the irradiation dose, as well as by varying the temperature along the melting line or by changing the angle between the columnar defects and the magnetic field.

The BSCCO crystals, with $T_c \simeq 90$ K, were grown by the traveling solvent zone method.[14] Several crystals with typical dimensions $500 \times 300 \times 10$ $\mu m^3$ were cut from one large single crystal of very high quality and uniformity and irradi-

ated at GANIL (Caen, France) by 5.8 GeV Pb ions parallel to the crystalline $c$ axis.[15] We have investigated very low irradiation doses corresponding to matching fields $B_\phi$ of 5, 10, 20, 30, 40, 50, and 100 G ($B_\phi = n\phi_0$, where $n$ is the density of the columns and $\phi_0$ is the flux quantum). The crystals were glued to the surface of a linear array of GaAs/AlGaAs Hall sensors[16] $10 \times 10$ $\mu m^2$ each, and mounted on a tiltable stage at the center of two orthogonal split-coil superconducting magnets. The stage is adjustable from outside the cryostat with an accuracy of about 0.1°, and the $c$ axis of the crystal was aligned parallel to one of the field components. The Hall sensors measure only the normal component, $B_z = B\cos\theta$, of magnetic induction, where $\theta$ is the angle between the induction and $c$ axis.

We describe first the results for field applied parallel to the columnar defects. Figure 1 shows the FOT and the corresponding step in the equilibrium magnetization for the as-grown crystal and for the crystal irradiated to a dose of $B_\phi = 20$ G. We find that for $B_\phi \lesssim 40$ G and for high enough temperatures, the FOT is preserved and the step in magnetization at $B_m(T)$ is resolved, as indicated by the arrow in Fig. 1. Above the transition the magnetization is fully reversible, indicating that the vortex fluid is not affected by such low doses of columns (on our experimental time scale). Below the transition, however, there is the hysteresis which increases significantly after irradiation. Due to the finite shear modulus, the vortex solid is effectively pinned even by a very low concentration of columnar defects, as described previously.[11,17] However, at these elevated temperatures the vortex-vortex interactions are still dominant, and thus the crystalline order of the vortex-lattice is sufficiently pre-
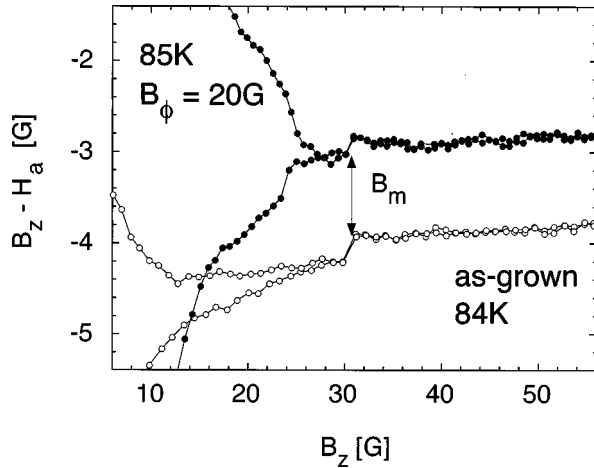
FIG. 1. Local magnetization loops $B_z - H_a$ vs $B_z$ in an as-grown BSCCO crystal (at $T = 84$ K) as compared to an irradiated crystal ($B_\phi = 20$ G, $T = 85$ K). $B_m$ indicates the position of the equilibrium magnetization step at the FOT in both crystals.

served. As a result, the lattice still melts through a FOT. In order to destroy the FOT, the pinning energy per unit volume has to be increased relative to the elastic energy or the shear modulus of the vortex lattice.[10,13] This can be achieved either by increasing the density of the columns or by moving to lower temperatures along the melting line and thereby increasing the pinning efficiency.

Figure 2 shows the effect of increasing $B_\phi$ at 60 K. For $B_\phi = 5$ G, the melting transition is visible; the local magnetization shows a sharp drop in the hysteresis at $B_m$ ($\theta = 0°$ data in Fig. 2), and the step in equilibrium magnetization can be resolved by a more detailed analysis as described below. However, for $B_\phi = 100$ G there is large hysteresis that extends to significantly higher fields ($B_{IB}$ in Fig. 2), and no features are observed at the original $B_m$. In this case the ordered vortex-lattice has transformed into a disordered state. The pinning potential lowers the free energy of the solid phase and stabilizes it with respect to the vortex fluid. As a
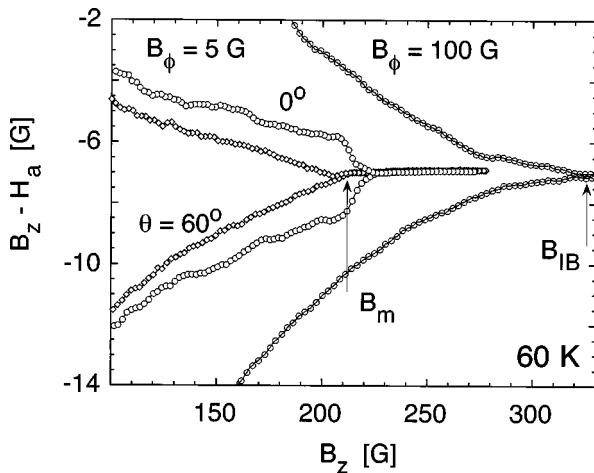


FIG. 2. Local magnetization loops $B_z - H_a$ vs $B_z$ ($T = 60$ K) of irradiated crystals with $B_\phi = 5$ G ($\theta = 0°$ and $60°$) and 100 G ($\theta = 0°$). For $B_\phi = 5$ G the FOT is observed at $B_m$. The bulk irreversibility field $B_{IB}$ for $B_\phi = 100$ G indicates the field above which the bulk pinning drops below our experimental resolution.
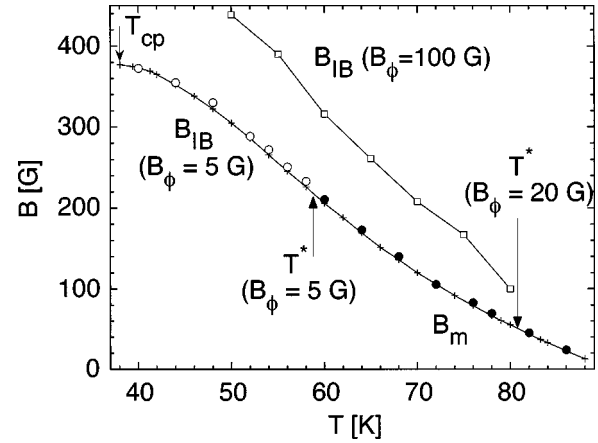


FIG. 3. FOT line $B_m(T)$ for the as-grown ($+$) and for the irradiated BSCCO crystal $B_\phi = 5$ G ($\bullet$) as determined by the equilibrium magnetization step. For $B_\phi = 5$ G, the bulk depinning line $B_{IB}(T)$ ($\bigcirc$) follows the as-grown $B_m(T)$ line for $T < T^*$. $T^*$ for $B_\phi = 20$ G is indicated for comparison. For $B_\phi = 100$ G, $B_{IB}(T)$ is shifted significantly above $B_m(T)$, in contrast to the behavior for $B_\phi \lesssim 40$ G. $T_{cp}$ is the critical point at which the FOT in the as-grown crystal terminates and below which the second magnetization peak transition appears (Refs. 16 and 11).

result, this disordered solid melts through a continuous transition at a higher field (or temperature) where the thermal energy becomes comparable to the pinning energy.[2,10] The shift of the resulting depinning or bulk irreversibility line $B_{IB}(T)$ of the disordered solid for $B_\phi = 100$ G, as compared to $B_m(T)$, is shown in Fig. 3.

An alternative way to transform the FOT into a continuous transition is by moving to lower temperatures along the melting line. With decreasing temperature, the step becomes harder to resolve because of enhanced pinning and hysteresis in the solid phase. We therefore apply the following, more sensitive analysis to determine the existence of the magnetization step. In a platelet geometry in the absence of bulk pinning, the induction across the sample $B_z(x)$ has a dome shaped profile.[18] As a result, vortex-lattice melting occurs first in the central part of the sample, forming a vortex fluid region surrounded by vortex solid.[19,20] At the interface, a sharp step $\Delta B$ in the induction $B_z(x)$ is present. In as-grown crystals, this step is readily observed directly as shown in Fig. 4(a). Alternatively, we can analyze $dB_z(x)/dx$. A step function in $B_z(x)$ produces a sharp peak in $dB_z(x)/dx$, which is a more sensitive way of detecting the FOT in the presence of enhanced pinning. This procedure is demonstrated in Fig. 4 by plotting the difference in inductions measured by two adjacent sensors.[18] A clear peak in $dB_z/dx$ is observed in both the as-grown and the irradiated sample. In addition, Fig. 4(b) shows that in the irradiated samples bulk pinning becomes significant immediately below the FOT, as reflected by the enhanced hysteresis in $dB_z(x)/dx$.[11,18]

Using the above procedure, we find that for $B_\phi = 5$ G the magnetization step is observable, as in Fig. 4(b), down to $T^* \simeq 59$ K, as shown by the solid circles in Fig. 3. At higher doses, $T^*$ increases due to the enhanced pinning and disorder, and for $B_\phi = 20$ G, $T^* \simeq 80$ K, as indicated by the arrow. At doses above $B_\phi = 40$ G we do not resolve the magnetization step at any temperature. The behavior at $T < T^*$ is rather
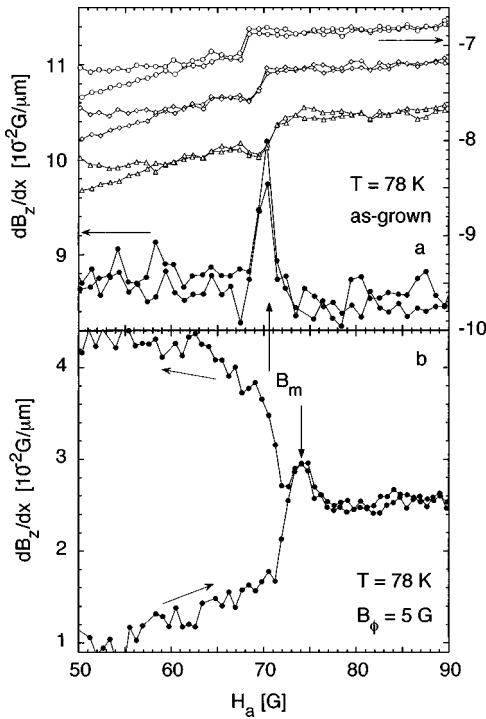
FIG. 4. (a) Three upper curves show the local magnetization loops $B_z - H_a$ and the FOT magnetization step for the as-grown crystal as measured by three adjacent sensors (vertically shifted for clarity). The solid-fluid interface moves toward the edges with increasing field and thus appears at higher $H_a$ for sensors closer to the edge. The lower curve (●) shows the corresponding $dB_z/dx$ obtained by differentiating the field measured by two adjacent sensors. The step in $B_z$ at melting manifests itself as a sharp peak in $dB_z/dx$ (indicated by $B_m$). (b) $dB_z/dx$ vs $H_a$ for the $B_\phi = 5$ G sample. The FOT is clearly observed as a peak in $dB_z/dx$.



FIG. 5. The apparent $J_c$ vs $B_z$ for the irradiated BSCCO crystal with $B_\phi = 5$ G at various angles ($0°$, $28°$, $45°$, and $60°$) of $H_a$ with respect to the columnar defects. At $\theta = 60°$ the pinning is sufficiently reduced and the equilibrium magnetization step at the FOT is restored, as seen by the peak in $dB_z/dx$ at the transition (encircled for clarity).

remarkable. In this region the equilibrium magnetization step is fully suppressed within our experimental resolution. Yet the solid-fluid transition line still follows the pristine $B_m(T)$ line, as shown by the $B_{IB}$ (open circles) in Fig. 3. We interpret this behavior as follows. The concentration of columnar defects is so low in our case that a vortex pinned on a column is surrounded on the average by 40 to 70 free vortices ($B \simeq 200-370$ G in Fig. 3, while $B_\phi = 5$ G). At $T > T^*$ the pinning of vortices by individual columns is smeared out by thermal fluctuations, and thus the elastic energy is dominant at low $B_\phi$. As a result, long-range order is preserved and the lattice melts through a FOT. At lower temperatures the pinning of the individual vortices becomes dominant. The random distribution of the columns destroys the long-range order, and thus the FOT is replaced by a continuous transition.[10] Yet, the relatively large domains of free vortices between the columns still melt at about $B_m(T)$, and the shear modulus of the entire lattice vanishes. Consequently, the unpinned vortices can readily move past the few vortices pinned on the columns, and thus the hysteresis and $J_c$ disappear abruptly (see Figs. 2 and 5 for $B_\phi = 5$ G and $\theta = 0°$). As a result, the bulk irreversibility $B_{IB}(T)$ follows the original $B_m(T)$ line. We observe this behavior up to irradiation doses of $B_\phi = 40$ G. For $B_\phi = 50$ G, $B_{IB}(T)$ shows a small upward shift with respect to $B_m(T)$ at intermediate temperatures;[21] for $B_\phi = 100$ G, a much more significant shift is obtained, as
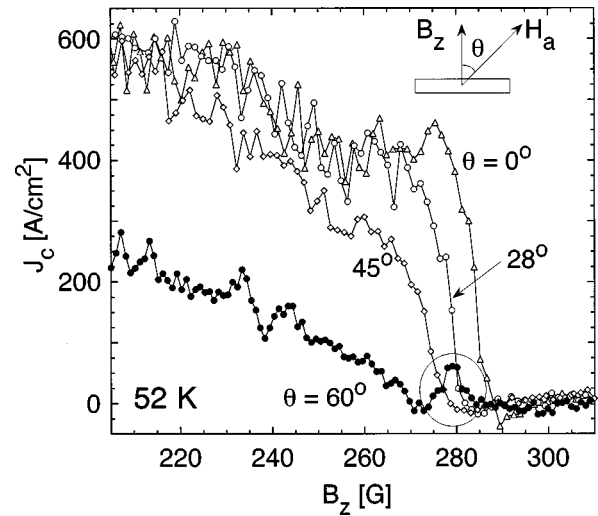
seen in Figs. 2 and 3. At these doses the density of columns becomes comparable to or larger than the density of vortices. Therefore, the vortices are pinned either by individual columns or at the intercolumn cites due to vortex-vortex interaction. As a result, the vortex-lattice transforms into a highly disordered glassy phase which melts through a continuous transition at higher temperatures.

The pinning efficiency of columnar defects can be reduced by tilting the magnetic field with respect to the columns, as shown by the change in the magnetic hysteresis in Fig. 2 ($B_\phi = 5$ G at $\theta = 0°$ and $60°$). Figure 5 shows the apparent critical current for $B_\phi = 5$ G and $T = 52$ K $< T^*$ at various tilt angles $\theta$. The apparent $J_c$ was derived from experimentally measured $B_z(x)$ profiles using the Bean-model calculation.[22,18] At $\theta = 0°$ a sharp drop in $J_c$ coincides with the as-grown $B_m(T)$. However, no step in equilibrium magnetization is observed at this $T < T^*$ (see Fig. 3). For tilting angles up to $45°$ the behavior is qualitatively the same. However, at larger angles, such as $60°$ (see Fig. 5), $J_c$ is reduced significantly and furthermore, the equilibrium magnetization step of the FOT reappears. The magnetization step is detected as a peak in $dB_z/dx$, encircled for clarity in Fig. 5, similar to the peak shown in Fig. 4 for the as-grown crystal and the irradiated sample at $T > T^*$.

At small angles the columns act as strong correlated disorder that results in substantial $J_c$ and in suppression of the FOT. As the angle is increased, progressively larger vortex segments reside outside the columns forming a staircase structure.[1,2] At sufficiently large angles ($\theta > 60°$) the columns apparently act more like point disorder which pins the vortices only at a few random intersection points. As a result, $J_c$ is reduced and the FOT is recovered. Since there are no reports of the effect of columnar defects on FOT, we can only compare our results with the effect of a low concentration of twin boundaries in YBa$_2$Cu$_3$O$_7$ (YBCO). It was shown that the resistive step at the FOT in lightly twinned YBCO is enhanced by tilting the field away from the twin

planes.[23] However, in YBCO the pinning accommodation angle of the twin boundaries is only on the order of $5°$, as compared to about $60°$ in our case. The difference can be ascribed to the more rigid lattice in YBCO due to lower anisotropy, and to a possibly weaker pinning potential of twin boundaries as compared to columnar defects. It is important to note that the typical field at the FOT in YBCO is two orders of magnitude larger than in BSCCO. In BSCCO, as well as in YBCO,[9] a very large accommodation angle of the columnar defects of up to $70°$ was shown.[5,7] Figure 5 shows that the behavior in the vicinity of the FOT at low $B_\phi$ is consistent with the reported angular dependence of pinning at much larger values of $B_\phi$.

We note that the melting transition shifts to lower $B_z$ with increasing tilt angle, as observed by the sharp drop in $J_c(B_z)$ for $\theta = 0°$, $28°$, and $45°$ in Fig. 5. The scaling theory of anisotropic superconductors[1] predicts that $B_m(\theta)$ scales as $B_m(\theta) = B_m(0)/(\cos^2\theta + \epsilon^2\sin^2\theta)^{1/2}$, where $\epsilon$ is the small anisotropy parameter. Since for BSCCO $\epsilon \lesssim 0.01$, in our range of tilt angles there should be no observable shift of the normal component of the melting field $B_m\cos\theta$ with $\theta$. Yet some experiments in BSCCO have shown substantially larger shifts of the melting field compared to the predicted scaling,[24] particularly at lower temperatures. Our results are consistent with those reports. The exact origin of this en-

hanced shift is not clear at present. It was shown that at lower temperatures point disorder causes a downward shift of the melting line in BSCCO (Refs. 11 and 21) because of disorder-induced wandering of the vortices which assists the thermal fluctuations in melting the lattice.[13,25] It is possible that point disorder also enhances the angular dependence of the melting line. In the presence of columnar defects this effect may become more pronounced since the columns act as additional point disorder at large angles.

In summary, we have studied the effect of low concentrations of columnar defects on the FOT in BSSCO. A concentration as low as one column per 70 vortices fully suppresses the equilibrium magnetization step at the transition at temperatures below $T^*$. Yet the solid-fluid transition line still follows the pristine melting line for $B_\phi \lesssim 40$ G. The FOT can be recovered by tilting the applied field with respect to the columns. Irradiation doses in excess of $B_\phi = 50$ G shift the solid-fluid transition to higher fields.

[1] G. Blatter *et al.*, Rev. Mod. Phys. **66**, 1125 (1994); E. H. Brandt, Rep. Prog. Phys. **58**, 1465 (1995).

[2] D. R. Nelson and V. M. Vinokur, Phys. Rev. B **48**, 13 060 (1993).

[3] L. Civale *et al.*, Phys. Rev. Lett. **67**, 648 (1991); M. Konczykowski *et al.*, Phys. Rev. B **44**, 7167 (1991); W. Gerhauser *et al.*, Phys. Rev. Lett. **68**, 879 (1992).

[4] M. Konczykowski *et al.*, Phys. Rev. B **51**, 3957 (1995); A. Samoilov *et al.*, Phys. Rev. Lett. **76**, 2798 (1996).

[5] L. Klein *et al.*, Phys. Rev. B **48**, 3523 (1993); R. C. Budhani *et al.*, Phys. Rev. Lett. **72**, 566 (1994); W. S. Seow *et al.*, Phys. Rev. B **53**, 14 611 (1996).

[6] R. A. Doyle *et al.*, Phys. Rev. Lett. **77**, 1155 (1996).

[7] C. J. van der Beek *et al.*, Phys. Rev. Lett. **74**, 1214 (1995).

[8] N. Morozov *et al.*, Phys. Rev. B **57**, R8146 (1998).

[9] L. M. Paulius *et al.*, Phys. Rev. B **56**, 913 (1997).

[10] A. I. Larkin and V. M. Vinokur, Phys. Rev. Lett. **75**, 4666 (1995).

[11] B. Khaykovich *et al.*, Phys. Rev. B **56**, R517 (1997).

[12] D. R. Nelson, Phys. Rev. Lett. **60**, 1973 (1988).

[13] V. M. Vinokur *et al.*, Physica C **295**, 209 (1998).

[14] N. Motohira *et al.*, J. Ceram. Soc. Jpn. **97**, 994 (1989).

[15] V. Hardy *et al.*, Nucl. Instrum. Methods Phys. Res. B **54**, 472 (1991).

[16] E. Zeldov *et al.*, Nature (London) **375**, 373 (1995).

[17] R. A. Doyle *et al.*, Physica C **282–287**, 323 (1997).

[18] E. Zeldov *et al.*, Europhys. Lett. **30**, 367 (1995).

[19] N. Morozov *et al.*, Phys. Rev. B **54**, R3784 (1996).

[20] A. I. M. Rae *et al.*, cond-mat/9708236 Physica C (to be published).

[21] B. Khaykovich *et al.*, Czech. J. Phys. **46**, Supl. S6 3218 (1996).

[22] E. H. Brandt and M. V. Indenbom, Phys. Rev. B **48**, 12 893 (1993); E. Zeldov *et al.*, *ibid.* **49**, 9802 (1994).

[23] W. K. Kwok *et al.*, Phys. Rev. Lett. **73**, 2614 (1994); **76**, 4596 (1996); Physica B **197**, 579 (1994).

[24] B. Schmidt *et al.*, Phys. Rev. B **55**, R8705 (1997); Y. Yamaguchi *et al.*, Physica C **273**, 261 (1997).

[25] D. Ertas and D. R. Nelson, Physica C **272**, 79 (1996).